HHS Public Access

Author manuscript

Free Radic Biol Med. Author manuscript; available in PMC 2020 April 01.

Published in final edited form as:

Free Radic Biol Med. 2019 April ; 134: 1–8. doi:10.1016/j.freeradbiomed.2018.12.029.

The Triangle of Death of Neurons: Oxidative Damage, Mitochondrial Dysfunction, and Loss of Choline-Containing Biomolecules in Brains of Mice Treated with Doxorubicin. Advanced Insights into Mechanisms of Chemotherapy Induced Cognitive Impairment ("Chemobrain") Involving TNF-α

Xiaojia REN[1,1], **Jeriel T. R. KEENEY**[1,1], **Sumitra MIRIYALA**[2], **Teresa NOEL**[2], **David K. POWELL**[3], **Luksana CHAISWING**[2], **Subbarao BONDADA**[5,6], **Daret K. ST. CLAIR**[2,4,5], and **D. Allan BUTTERFIELD**[1,5,7,*]

[1]Department of Chemistry, University of Kentucky, Lexington, KY 40506, USA

[2]Department of Toxicology and Cancer Biology, University of Kentucky, Lexington, Kentucky 40536, USA

[3]Magnetic Resonance Imaging and Spectroscopy Center, University of Kentucky Medical Center, Lexington, KY 40536, USA

[4]Department of Radiation Medicine, University of Kentucky, Lexington, KY 40536

[5]Markey Cancer Center, University of Kentucky, Lexington, KY 40536 USA

[6]Department of Microbiology, Immunology & Molecular Genetics, University of Kentucky, Lexington, KY 40536

[7]Sanders-Brown Center on Aging, University of Kentucky, Lexington, KY 40536

Abstract

Cancer treatments are developing fast and the number of cancer survivors could arise to 20 million in United State by 2025. However, a large fraction of cancer survivors demonstrate cognitive dysfunction and associated decreased quality of life both shortly, and often long-term, after chemotherapy treatment. The etiologies of chemotherapy induced cognitive impairment (CICI) are complicated, made more so by the fact that many anti-cancer drugs cannot cross the blood-brain barrier (BBB). Multiple related factors and confounders lead to difficulties in determining the underlying mechanisms. Chemotherapy induced, oxidative stress-mediated tumor necrosis factor-alpha (TNF-α) elevation was considered as one of the main candidate mechanisms underlying CICI. Doxorubicin (Dox) is a prototypical reactive oxygen species (ROS)-generating chemotherapeutic agent used to treat solid tumors and lymphomas as part of multi-drug

*To whom correspondence should be addressed: Prof. D. Allan Butterfield Dept. of Chemistry, Markey Cancer Center, and Sanders-Brown Center on Aging University of Kentucky, Lexington, KY 40506 USA Ph: 859-257-3184; dabcns@uky.edu.
[1]Co-First Authors

chemotherapeutic regimens. We previously reported that peripheral Dox-administration leads to plasma protein damage and elevation of TNF-α in plasma and brain of mice. In the present study, we used TNF-α null (TNFKO) mice to investigate the role of TNF-α in Dox-induced, oxidative stress-mediated alterations in brain. We report that Dox-induced oxidative stress in brain is ameliorated and brain mitochondrial function assessed by the Seahorse-determined oxygen consumption rate (OCR) is preserved in brains of TNFKO mice. Further, we show that Dox-decreased the level of hippocampal choline-containing compounds and brain phospholipases activity are partially protected in TNFKO group in MRS study. Our results provide strong evidence that Dox-targeted mitochondrial damage and levels of brain choline-containing metabolites, as well as phospholipases changes decreased in the CNS are associated with oxidative stress mediated by TNF-α.

These results are consistent with the notion that oxidative stress and elevated TNF-α in brain underlie the damage to mitochondria and other pathological changes that lead to CICI. The results are discussed with reference to our identifying a potential therapeutic target to protect against cognitive problems after chemotherapy.

Keywords

Doxorubicin; MRS; chemotherapy-induced cognitive impairment; phospholipases; mitochondrial dysfunction; oxidative stress; tumor necrosis factor-alpha

1. Introduction

Cancer survivors often lose, at least in part, cognitive abilities of concentration, attention, learning and memory, and executive functions. Such patients often describe feelings of “chemofog” and feel it difficult to remember details, as well as slowness in problem-solving and multitasking. These symptoms are characteristic of as chemotherapy induced cognitive impairment (CICI). CICI could acutely or chronically happen to cancer survivors who had chemotherapy history and negatively affect their quality of life. However, many chemotherapeutical drugs are not able to cross the blood-brain barrier (BBB), but still can result in the injury to the CNS and lead to cognitive deficits. The mechanisms of CICI remain unclear. Although it is difficult to clarify the precise mechanisms of CICI, many candidates have been put forward, one of which is oxidative stress mediated elevation of pro-inflammatory cytokines [1, 2].

Approximately half of FDA approved anti-cancer drugs are known to generate reactive oxygen species (ROS) resulting in oxidative stress [3]. Doxorubicin (Dox), an anti-neoplastic anthracycline and one of these non-BBB-penetrating drugs, is used primarily to treat solid tumors and lymphomas as part of multi-drug chemotherapy regimens. In the presence of oxygen, the redox cycling of Dox between the quinone and semi-quinone forms results in production of superoxide radical anion ($O_2^{-}\bullet$) [4–6]. Dox-induced oxidation of plasma-resident ApoA1 and resulting elevation of plasma levels of TNF-α that is transported to the brain are thought to be independent of its antitumor ability [7–9]. Oxidative and nitrosative damage in the brain occur despite the inability of Dox to cross the BBB [10–15].

Mitochondrial dysfunction induced by Dox has been well established, especially in the heart [16–18]. Cardiac toxicity is the dose-limiting factor in Dox treatment [14]. Prior studies by our groups demonstrated that Dox-induced mitochondrial dysfunction also occurs in brain via a mechanism involving nitration of the mitochondrial $O_2^{-\bullet}$ scavenger, manganese superoxide dismutase (MnSOD) [14]. TNF-α and inducible nitric oxide synthase (iNOS) are both downstream products of the nuclear factor κ-light-chain enhancer of activated B-cells (NF-κB) pathway [19, 20]. Mitochondrial ROS are thought to be involved in the activation of this pathway [21]. Meanwhile, the volume of the hippocampus, important to learning and memory, and neurogenesis are affected by TNF-α [22, 23], leading to behavioral deficits [24] such as anxiety and depressive-like behaviors, considered as chemotherapy induced symptoms as well. Peripherally elevated TNF-α can cross the BBB via receptor-mediated endocytosis to elicit microglial activation resulting in further TNF-α release in brain [2]. Therefore, Dox-induced mitochondrial dysfunction likely is associated with TNF-α, resulting in apoptosis [3,13] and ultimately in cognitive decline of cancer survivors.

In the current study, we tested the hypothesis that TNF-α underlies alterations in brain measures of oxidative stress, hippocampal neurochemical profiles, phospholipase C and D activities, and mitochondrial function in wild type (WT), but not TNF-α null (TNFKO) mice following *in vivo* Dox administration. The results support this hypothesis.

2. Methods and Materials

2.1 Chemicals

BCA reagents, and nitrocellulose membranes were purchased from Bio-Rad (Hercules, CA, USA). All chemicals, protease, protease inhibitors and antibodies were purchased from Sigma-Aldrich (St. Louis, MO, USA) unless otherwise noted. EnzChek® Direct Phospolipase C Assay Kit and Amplex® Red Phospholipase D Assay Kit were purchased from Invitrogen/Life Technologies (Carlsbad, CA, USA).

2.2 Statistical analysis

ANOVA was performed followed by a two-tailed Student's t-test to make individual comparisons between groups using GraphPad Prism 5 software. All data are presented as mean±SEM and $p<0.05$ is considered as a significant difference relative to the appropriate control. The D'Agostino & Pearson omnibus normality test was used where appropriate.

2.3 Animals

All procedures were approved by the Institutional Animal Care and Use Committee of the University of Kentucky in accordance with the U.S. National Institutes of Health Guide for the Care and Use of Laboratory Animals. The animals were housed following standard conditions in an air-conditioned environment (22.1°C, 50.5% relative humidity, 12 h light-dark cycle), with free access to food and water, in the University of Kentucky Animal Care Facility. Male, WT B6C3F1/J (B6C3) and B6.129S6-*Tnf*^{tm1Gkl}/J (TNF-α knockout, TNFKO) mice were purchased from the Jackson Laboratory. Doxorubicin HCl was purchased from Bedford Laboratories™. Mice were 2–3 months old and each weighing approximately 25–30 grams. Mice were injected using a single intraperitoneal (i.p.) dose of

25mg/kg Dox or the same volume of saline as a control. MRS was performed 72 h post treatment using methods described below. Following MRS studies, animals were euthanized and blood and tissues collected for molecular or biochemical analysis.

2.4 Sample preparation

Bicinchoninic acid (BCA, Pierce) assay [25] was used for protein quantification. BCA protein assay reagent A and B were purchased from Thermo Fisher Scientific (Waltham, MA, USA). Homogenized brain and plasma samples were diluted according to initial protein estimation results using 20 ug sample in isolation buffer [0.32 M sucrose, 2 mM EDTA, 2mM EGTA, and 20mM HEPES pH 7.4 with protease inhibitors, 0.2 mM PMSF, 20ug/mL trypsin inhibitor, 4 μg/ml leupeptin, 4 μg/ml pepstatin A, and 5 μg/ml aprotinin].

2.5 Slot blot assay

Protein carbonyls (PC) and protein-bound 4-hydroxy-2-*trans*-nonenal (HNE) were detected by slot blot assay [8, 26]. For PC determination, samples were derivatized with 2,4-dinitrophenylhydrazine (DNPH). For HNE, samples were solubilized in Laemmli buffer. Protein (250 ng) from each sample was loaded onto a nitrocellulose membrane in respective wells in a slot-blot apparatus (Bio-Rad, Hercules, CA, USA) under vacuum built by water suction system. Membranes were blocked in 3% bovine serum albumin (BSA) in PBS with 0.2% (v/v) Tween-20 for 1.5 h and then incubated in primary antibody (anti-dinitrophenylhydrazone primary or anti-protein-bound HNE, respectively, each produced in rabbit, Sigma-Aldrich) for 2 h, washed three times in PBS with 0.2% (v/v) Tween-20 and then incubated for 1 h with secondary antibody (goat anti-rabbit secondary linked to alkaline phosphatase). Membranes were developed for alkaline phosphatase activity (ALP) buffer containing 5-bromo-4-chloro-3-indolyl-phosphate (BCIP) dipotassium and nitro blue tetrazolium (NBT) chloride, and then dried overnight, followed with image scanning for analysis performed using Scion Image (Scion Corporation, Frederick, MD). Specificity of each antibody used was demonstrated by the lack of signal for PC and HNE if the carbonyl groups on proteins were reduced by sodium borohydride to the respective alcohols.

2.6 Isolation of Brain Mitochondria

Mice were perfused via cardiac puncture with cold mitochondrial isolation buffer, the brain promptly removed, the cerebellum dissected away, and the mitochondria immediately isolated from the brain by a modification of the method described by Mattiazzi et al. [27]. Brain mitochondria were isolated in cold mitochondrial isolation buffer, containing 0.07 M sucrose, 0.22 M mannitol, 20 mM HEPES, 1 mM EGTA, and 1% bovine serum albumin, pH 7.2. Tissues were homogenized with a Dounce homogenizer and centrifuged at 1500 × g at 4°C for 5 min before transferring the supernatants. The pellets were resuspended and centrifuged at 1500 × g at 4°C for 5 min. The supernatants were combined and recentrifuged at 1500 × g at 4°C for 5 min. The supernatants were separated and centrifuged at 13,500 × g at 4°C for 10 min. Mitochondrial pellets were purified with 4% Ficoll solution and the mitochondrial pellet was resuspended in 50 μL cold mitochondrial isolation buffer. Protein concentration of isolated mitochondria was determined by the Bradford assay [25].

2.7 Bioenergetic analysis in mitochondria

The XF96 Analyzer, Agilent (Santa Clara, CA, USA) was used to measure bioenergetic function in mitochondria freshly isolated by differential centrifugation from brain of adult male C57BL6 mice. The XF96 creates a transient 3μl chamber in specialized microplates that allows for the measurement of oxygen consumption rate (OCR) in real time. Respiration by the mitochondria (5 μg/well) was sequentially measured with substrate present (basal respiration) following conversion of ADP to ATP, induced with the addition of oligomycin. Next, maximal uncoupler-stimulated respiration was detected by the administration of the uncoupling agent FCCP. At the end of the experiment, the complex III inhibitor, antimycin A, was applied to completely inhibit mitochondrial respiration. Oxygen consumption rates were measured at four time points with three replicates and plotted as a function of cells, showing the relative contribution of oxygen consumption, ATP-linked oxygen consumption, the maximal OCR after the addition of FCCP, and the reserve capacity of the cells.

2.8 Hydrogen magnetic resonance spectroscopy

H^1-MRS (hydrogen magnetic resonance spectroscopy) was used to quantify neurochemical changes in the mouse hippocampus. MRS data was acquired on a 7T BrukerClinscan horizontal bore system (7.0T, 30cm, 300Hz) equipped with a triple-axis gradient system (630 mT/m and 6300 T/m/s). A closed cycle, 14K quadrature cryocoil allowed for a 2.8 signal to noise increase relative to standard coils. Isoflurane (1.3%) was used to anesthetize mice before scanning mice in MRI compatible CWE Inc. equipment. Mice were placed on a Bruker scanning bed with a tooth bar, ear bars and tape. Body temperature and respiration rate were monitored using equipment from SA Instruments Inc. The water heating system for the scanning bed maintained mice body temperature at 37°C. T2 weighted turbo spin echo sequences (TE 40ms, TR 2890ms, Turbo 7, FOV 20mm, $0.156 \times 0.156 \times 5.0\ mm^3$) were acquired and used for the placement of the spectroscopy voxel. The scanning procedure took 40 min. A $2 \times 5.5 \times 3 mm^3$ PRESS spectroscopic voxels (TE 135ms, TR 1500ms, 400avg, CHESS water suppression) was placed to cover both hippocampi. Spectrum analysis was performed using jMRUI [28] to quantify the areas under 10 individual peaks in the MRS spectrum. The area of the creatine (Cr) peak was used to normalize the area of peaks of all other metabolites.

2.9 Phospholipase C and Phospholipase D Activity Assays

Phosphatidylcholine-specific phospholipase C (PC-PLC) and phospholipase D (PLD) activity assays were performed using manufacturers' instructions provided with the EnzChek® Direct Phospolipase C Assay Kit and Amplex® Red Phospholipase D Assay Kit by Invitrogen/Life Technologies (Carlsbad, CA). A SPECTRAFLUOR PLUS instrument was used to determine the fluorescence, quantified by Magellan™ software. The kinetic peaks of fluorescence of positive control were recorded over a period of 24h. The samples' fluorescence were acquired at incubation time at the peak.

3. Results

3.1 Dox administration results in increased oxidative stress markers in brain and plasma of WT mice that is absent in brain of TNFKO mice

Dox administration causes increased global oxidative stress in plasma and brain [7, 12, 29] as well as oxidative damage to key plasma and brain proteins, including peripheral oxidized Apoprotein A-1 that leads to elevated TNF-α in plasma [7, 10, 12, 13, 30]. Peripheral TNF-α crosses the blood-brain barrier leading to oxidative damage in brain and apoptotic brain cell death [7, 10, 12, 13, 30]. Consequently, to test the hypothesis that TNF-α is the principal cytokine elevated in plasma following Dox treatment that leads to brain oxidative and mitochondrial damage and resulting apoptotic cell death, we investigated the effects of Dox administration on oxidative damage in plasma and brain in TNF-α knockout (TNFKO) mice. Test subjects were administered either saline or Dox. Samples were collected at approximately 72 h post-Dox treatment, immediately following MRS studies. PC levels were used as a gauge of protein oxidation, while the lipid peroxidation product, protein-bound HNE, was used as an index of lipid damage.

Dox administration resulted in elevation of oxidative stress markers, PC and protein-bound HNE, in both plasma and brain of WT mice (Fig. 1a–d, **P<0.01, **P<0.01, ****P<0.0001, and *P<0.05, respectively). Due to its redox cycling properties associated with the quinone moiety in this anthracycline drug, Dox-treated TNFKO mice still exhibited elevated PC levels and protein-bound HNE in plasma compared to saline-treated TNFKO mice (**p<0.01, Fig. 1a and *p<0.05, Fig. 1c, respectively); however, in brain of TNFKO mice, PC and protein-bound HNE levels following Dox treatment were found not to be significantly different from levels observed in saline-treated TNFKO mice (Fig. 1b and Fig. 1d). This result is strong evidence to support our hypothesis that TNF-α plays a central role in Dox-induced oxidative stress in brain.

3.2 Dox administration results in altered oxygen consumption rate in WT mice brain mitochondria that is prevented in TNFKO mice

Prior studies using a Clarke-type electrode demonstrated TNF-α-mediated mitochondrial dysfunction as assessed by oxygen utilization in brain as a consequence of peripheral Dox administration [13–15]. In the present study and shown in Figure 2, we measured mitochondrial oxygen consumption rate (OCR) in mitochondria isolated from brain of saline-treated WT (blue circles), Dox-treated WT (red squares), saline-treated TNFKO (purple x’s), and Dox-treated TNFKO (green triangles) mice (Fig. 2a). Basal, ATP-linked, maximal capacity, and reserve capacity OCR (related to ATP production) were ascertained in fresh brain mitochondria of each treatment group (Fig. 2b).

We observed a significant decline in mitochondrial respiration in brain of Dox-treated WT mice as indexed by mitochondrial OCR. Compared to saline-treated WT mice, Dox-treated WT mice significantly exhibited decreased mitochondrial OCR at every phase measured (Fig. 2b; basal, p<0.01; ATP-linked, p<0.01; maximal capacity, p<0.0001; reserve capacity, p<0.005). Compellingly, mitochondrial OCR observed in brain of Dox-treated TNFKO mice was similar to that observed in brain of saline-treated WT and saline-treated TNFKO mice at

every phase of mitochondrial OCR measured (Fig. 2b). This result supports our hypothesis that TNF-α is a key player in the observed mitochondrial dysfunction in brain from WT mice following Dox administration.

3.3 Changes to the neurochemical profile in hippocampus following Dox administration

Bilateral H^1-MRS scans of hippocampus revealed a dramatic decrease in the ratio of peak area of Choline-containing compounds (Cho) to that of Cr in Dox-treated WT mice compared to that in saline-treated control WT mice (Figure 3, ****p<0.0001) confirming our earlier studies with WT mice [31]. The Cho/Cr ratio in Dox-treated TNFKO mice brain was still lower than that observed in saline-treated TNFKO mice (****P<0.0001), but profoundly higher than that (the Cho/Cr in brain) of Dox-treated WT mice (***p=0.0002), showing significant protection in the Cho/Cr ratio in mice hippocampus if TNF-α were absent. This result also provides strong evidence of TNF-α involvement in the Dox-induced decreased Cho/Cr ratio in brain.

3.4 Dox administration to TNFKO mice results in partial preservation of PLD activity

Dox administration to WT mice resulted in significant decreased activities of both PCPLC and PLD in mouse hippocampus that likely contribute to the loss of Cho/Cr as determined by MRS [31]. The protection of the Cho/Cr ratio in the hippocampus of TNFKO mice observed by MRS (Fig. 3) led to examination of the effect of TNF-α on activities on phospholipases responsible for the cleavage of choline and phosphocholine from PtdCho. Dox administration resulted in decreased activity of PCPLC (Fig. 4a) in brain of WT mice compared to saline-treated WT mice (****P<0.0001). Dox also led to a decreased activity of PC-PLC in TNFKO mice compared to saline-treated TNFKO mice (****P<0.0001), the results did not show any protection on PC-PLC activity in TNFKO mice following Dox treatment. As shown in Fig. 4b, Dox administration resulted in significant decreased activity of PLD in brain of mice in both WT and TNFKO groups, compared to saline-treated WT (****P<0.0001) and TNFKO (***P=0.0005) mice, respectively. However, a significant difference on PLD activity in mice brain also existed between the Dox-treated WT group and the Dox-treated TNFKO group (***P=0.0008), which indicated that brain PLD activity in TNFKO mice was protected from loss following Dox administration, but not completely. The results are consistent with the notion that TNF-α plays an important role in diminution of PLD activity following Dox treatment.

4. Discussion

Many chemotherapy patients experience cognitive deficits following chemotherapy [32], and as the number of cancer survivors increase with improved treatment, CICI should be taken into account so the quality of life after cancer treatment is not materially affected. Understanding the mechanisms of etiology and pathogenesis of CICI is necessary for prevention strategies for this condition. We propose that TNF-α, one of the chemotherapy induced, oxidative stress associated, pro-inflammatory cytokines, plays a crucial role in CICI. Accordingly, the TNF-α knock-out animal model is an important and useful tool to investigate the hypothesized central role of TNF-α in CICI.

Dox is used in our laboratory as a prototypical ROS-generating chemotherapeutic agent that does not cross the BBB to investigate CICI. Dox administration led to damage with significantly increased oxidative stress and TNF-α elevation in both plasma and brain [7, 13–15, 29]. The resultant CNS injury included damage to key antioxidant enzymes, mitochondrial dysfunction, neuronal death, and cognitive dysfunction [10, 13, 14, 31]. Poor performance on the novel objective recognition tests of mice [31] and passive avoidance tests of rats [33] following Dox administration demonstrated that this ROS-generating chemotherapeutic agent leads to learning and memory deficits in rodents that mimics cognitive changes in CICI.

In the current study, we observed that oxidative damage to proteins and lipids present in plasma and brain of Dox-treated WT mice was also present in plasma of Dox-treated TNFKO mice (Fig. 1a, 1c), but not different than control in brain of the latter (Fig. 1b, 1d). That oxidative damage still can occur in the periphery with absence of TNF-α is consistent with the characteristics of Dox, generating superoxide free radicals via redox cycling of its quinone moiety in the presence of oxygen. The absence of oxidative damage in TNFKO mice brain following Dox treatment provides stronger evidence that TNF-α is a key player in elevation of Dox-induced oxidative stress in brain of WT mice.

One of the most detrimental consequences in brain following chemotherapy is damage to mitochondrial function [10, 13–15]. Evidence exists of mitochondrial dysfunction as a potential causal factor in a variety of neurodegenerative disorders, including Alzheimer disease, Parkinson disease, amyotrophic lateral sclerosis, and Huntington disease among others [1, 34, 35]. The brain has a high and constant energy requirement coupled with low energy stores. Mitochondria are responsible for meeting much of this energy demand [36]. Impairment of mitochondrial function in brain indexed by a decrease in Complex I activity of the electron transport chain following systemic Dox administration has been observed [13]. Here, using Seahorse technology, we explored the effect of Dox administration on mitochondrial respiration indexed by OCR (Fig. 2). Peripheral Dox-treatment resulted in decreased mitochondrial basal, ATP-linked OCR as well as reduced OCR maximal and reserve capacities in brain of WT mice (red, Fig. 2b). Strikingly, mitochondrial OCR in brain of Dox treated TNFKO mice (purple, Fig. 2) was preserved, equivalent to the level of that observed in saline-treated WT and TNFKO mice (blue and green, Fig. 2), indicating a central role of TNF-α in the decreased mitochondrial function in brain present following Dox administration. Once Dox-induced, TNF-mediated dysfunction of brain mitochondria happens, opening of the mitochondrial permeability transition pore associated with the observed loss of cytochrome c and elevated apoptotic brain cell death [13] likely underlies the loss of cognitive ability in mice following Dox administration [31].

H^1-MRS allows non-invasive measurement of neurochemical changes in living brain [37]. Previously, we observed changes in the neurochemical profile indexed by MRS in brain of WT mice following Dox administration [31]. Dox-treatment resulted in dramatic decreased ratio of Cho/Cr in the hippocampus, a brain region critically involved in learning and memory [38–41], and whose volume could be affected by Dox induced TNF-α [24]. In H^1-MRS, choline, phosphocholine (PCho) and glycerophosphorylcholine (GPC) contribute to a cluster of peaks representing Cho [31]. Elevated TNF-α reportedly inhibits synthesis of

PtdCho, a major source of Cho, PCho, and GPC in the brain [42, 43]. In the current study, bilateral hippocampal H^1-MRS showed profound a decreased Cho/Cr ratio at 72 h following Dox treatment of WT mice (Fig. 3), while similar MRS measurements in brain of TNFKO mice showed a significant rebound of the Cho/Cr ratio from levels observed in Dox-treated WT mice (Fig. 3). Changes in choline-containing compounds on MRS are thought to be associated with membrane turnover (phospholipid synthesis and degradation) [44, 45] and have been attributed to myelin damage following chemotherapy [46]. The absence of TNF-α afforded significant protection of the Cho/Cr ratio in brain suggesting involvement of TNF-α in neuronal membrane damage.

In order to gain further insight into the involvement of TNF-α in the decreased Dox-mediated Cho/Cr ratio indexed in brain by MRS and a potential contributor to mechanisms of CICI, in the current study the activities of phospholipases responsible for the cleavage of choline and phosphocholine from PtdCho in the brain in TNFKO mice were investigated. Activities of both PC-PLC and PLD were found to be significantly diminished in brain of Dox-treated WT mice at 72 h post-treatment (Fig. 4), confirming prior studies [31]. PC-PLC activity remained lowered in brain of Dox-treated TNFKO mice, while PLD activity was significantly higher in brain of TNFKO mice following Dox treatment, providing evidence of TNF-α involvement in Dox-induced inhibition of PLD activity. Although Dox does not cross the BBB, Dox-induced ROS in the periphery possibly leads to the oxidative impairment of the BBB, allowing small amount of Dox go into brain with local TNF-α elevation [47, 48], as well as brain oxidative stress (Fig. 1).

Reportedly, *PLCδ1* is a target gene for TNF receptor–mediated protection against cardiac injury by Dox [49]. Expression of PLCδ1 was decreased in TNF receptor knockout mice with Dox treatment [56], a result that conceivably could contribute to the observation of the current study that PC-PLC still shows a lower level in brain of the Dox-treated TNFKO group. In recent research, leptin-induced TNF-α elevation reportedly occurs through activation of PLD [50], suggesting that PLD is possibly affected more than PLC by TNF-α deficiency, consistent with our present findings using TNFKO mice. Moreover, phosphatidic acid, an intermediate of the PLD pathway, stimulated Ca^{2+}-mobilization and displayed growth factor-like activity [51], which could help decrease Dox-induced mitochondrial dysfunction in TNFKO mice brain. We opine this observation might contribute to the partial rescue of PLD in TNFKO mice. On the other hand, as noted, PLD also affects the level of TNF-α, consistent with the notion that PLD inhibition could lead to less cytokine production, including that of TNF-α [52–54]. Consonant with this idea, PLD was recently shown to be involved in TNF-α regulation by improving survival and decreasing TNF-α following LPS treatment in PLD knockout mice [53]. Further supporting this concept, LPS induced TNF-α elevation in mouse macrophage-like cells could be partially decreased by inhibition of PC-PLC or PC-PLD and completely blocked by inhibition of both phospholipases [54].

In addition to TNF-α-related inhibition of PtdCho biosynthesis [42], TNF-α has been linked to decline in phosphatidic acid levels [55]. PLD activity as well as the mRNA message for *PLD* have been shown to be increased during cellular differentiation and decreased during apoptosis [56, 57]. Enzymatic activity of PLD was seen as essential to cell survival, and

structural damage to PLD and decreased PLD activity are thought to promote apoptotic events [58, 59]. There could be a cross talk between the phospholipases and TNF-α expression due to their mutual dependence. Consequently, our results are consistent with the notion that ROS-generating chemotherapy agents' involvement in PLD inhibition potentially makes a significant contribution to CICI.

5. Conclusion

This study, to our knowledge, is the first to demonstrate that, in the absence of *TNF-α* MRS-indexed Cho/Cr ratio, PLD activity, and mitochondrial oxygen consumption rate are largely preserved in brain, and markers of elevated oxidative stress in brain absent following peripheral Dox treatment. Together, these results provide compelling evidence for the central role TNF-α in chemotherapy-induced mitochondrial neuronal damage and likely in the mechanisms of CICI (Fig. 5). Studies to gain further insights into CICI are in progress.

Acknowledgments

We thank the Redox Metabolism Shared Resource Facility of the NCI-designated Markey Cancer Center and its associated CCSG grant, 2 P30 CA177558–06 for the OCR results. This work was supported in part by a Multiple PI R01 grant to DAB, D.S.C., and S.B. [R01 CA217934–02].

Abbreviations:

CICI	Chemotherapy-induced cognitive impairment
ApoA-I	apolipoprotein A-I
Dox	Doxorubicin
OCR	oxygen consumption rate
MRS	magnetic resonance spectroscopy
PLC	phospholipase C
PLD	phospholipase D
PtdCho	phosphatidylcholine
PC-PLC	phosphatidylcholine-specific phospholipase C
TNF-α	tumor necrosis factor alpha
PC	protein carbonyl
HNE	4-hydroxy-2-*trans*-nonenal
BSA	bovine serum albumin
BCA	bicinchoninic acid
BCIP	5-bromo-4-chloro-3-indolyl-phosphate dipotassium

NBT	nitroblue tetrazolium chloride
ALP	alkaline phosphatase
BBB	blood-brain barrier
ROS	reactive oxygen species
O2−•	superoxide radical anion
Cho	Choline-containing compounds
Cr	creatine
GPC	glycerophosphorylcholine
PCho	phosphocholine
WT	wild-type

References

[1]. Butterfield DA, The 2013 SFRBM discovery award: selected discoveries from the butterfield laboratory of oxidative stress and its sequela in brain in cognitive disorders exemplified by Alzheimer disease and chemotherapy induced cognitive impairment, Free Radic Biol Med 74 (2014) 157–74. [PubMed: 24996204]

[2]. Ren X, St Clair DK, Butterfield DA, Dysregulation of cytokine mediated chemotherapy induced cognitive impairment, Pharmacol Res 117 (2017) 267–273. [PubMed: 28063894]

[3]. Chen Y, Jungsuwadee P, Vore M, Butterfield DA, St Clair DK, Collateral damage in cancer chemotherapy: oxidative stress in nontargeted tissues, Molecular interventions 7(3) (2007) 147–56. [PubMed: 17609521]

[4]. Bachur NR, Gordon SL, Gee MV, Anthracycline antibiotic augmentation of microsomal electron transport and free radical formation, Molecular pharmacology 13(5) (1977) 901–10. [PubMed: 19695]

[5]. Cummings J, Anderson L, Willmott N, Smyth JF, The molecular pharmacology of doxorubicin in vivo, Eur J Cancer 27(5) (1991) 532–5. [PubMed: 1647181]

[6]. Handa K, Sato S, Generation of free radicals of quinone group-containing anti-cancer chemicals in NADPH-microsome system as evidenced by initiation of sulfite oxidation, Gann = Gan 66(1) (1975) 43–7. [PubMed: 239881]

[7]. Aluise CD, Miriyala S, Noel T, Sultana R, Jungsuwadee P, Taylor TJ, Cai J, Pierce WM, Vore M, Moscow JA, St Clair DK, Butterfield DA, 2-Mercaptoethane sulfonate prevents doxorubicin-induced plasma protein oxidation and TNF-alpha release: implications for the reactive oxygen species-mediated mechanisms of chemobrain, Free Radic Biol Med 50(11) (2011) 1630–8. [PubMed: 21421044]

[8]. Bernacki RJ, Bansal SK, Gurtoo HL, Combinations of mesna with cyclophosphamide or adriamycin in the treatment of mice with tumors, Cancer research 47(3) (1987) 799–802. [PubMed: 3100025]

[9]. Hayslip J, Dressler EV, Weiss H, Taylor TJ, Chambers M, Noel T, Miriyala S, Keeney JT, Ren X, Sultana R, Vore M, Butterfield DA, St Clair D, Moscow JA, Plasma TNF-alpha and Soluble TNF Receptor Levels after Doxorubicin with or without Co-Administration of Mesna-A Randomized, Cross-Over Clinical Study, PLoS One 10(4) (2015) e0124988. [PubMed: 25909710]

[10]. Joshi G, Aluise CD, Cole MP, Sultana R, Pierce WM, Vore M, St Clair DK, Butterfield DA, Alterations in brain antioxidant enzymes and redox proteomic identification of oxidized brain proteins induced by the anti-cancer drug adriamycin: implications for oxidative stress-mediated chemobrain, Neuroscience 166(3) (2010) 796–807. [PubMed: 20096337]

[11]. Aluise CD, Sultana R, Tangpong J, Vore M, St Clair D, Moscow JA, Butterfield DA, Chemo brain (chemo fog) as a potential side effect of doxorubicin administration: role of cytokine-induced, oxidative/nitrosative stress in cognitive dysfunction, Advances in experimental medicine and biology 678 (2010) 147–56. [PubMed: 20738017]

[12]. Joshi G, Hardas S, Sultana R, St Clair DK, Vore M, Butterfield DA, Glutathione elevation by gamma-glutamyl cysteine ethyl ester as a potential therapeutic strategy for preventing oxidative stress in brain mediated by in vivo administration of adriamycin: Implication for chemobrain, Journal of neuroscience research 85(3) (2007) 497–503. [PubMed: 17171703]

[13]. Tangpong J, Cole MP, Sultana R, Joshi G, Estus S, Vore M, St Clair W, Ratanachaiyavong S, St Clair DK, Butterfield DA, Adriamycin-induced TNF-alpha-mediated central nervous system toxicity, Neurobiology of disease 23(1) (2006) 127–39. [PubMed: 16697651]

[14]. Tangpong J, Cole MP, Sultana R, Estus S, Vore M, St Clair W, Ratanachaiyavong S, St Clair DK, Butterfield DA, Adriamycin-mediated nitration of manganese superoxide dismutase in the central nervous system: insight into the mechanism of chemobrain, J Neurochem 100(1) (2007) 191–201. [PubMed: 17227439]

[15]. Tangpong J, Sompol P, Vore M, St Clair W, Butterfield DA, St Clair DK, Tumor necrosis factor alpha-mediated nitric oxide production enhances manganese superoxide dismutase nitration and mitochondrial dysfunction in primary neurons: an insight into the role of glial cells, Neuroscience 151(2) (2008) 622–9. [PubMed: 18160224]

[16]. Chen Y, Daosukho C, Opii WO, Turner DM, Pierce WM, Klein JB, Vore M, Butterfield DA, St Clair DK, Redox proteomic identification of oxidized cardiac proteins in adriamycin-treated mice, Free Radic Biol Med 41(9) (2006) 1470–7. [PubMed: 17023274]

[17]. DeAtley SM, Aksenov MY, Aksenova MV, Jordan B, Carney JM, Butterfield DA, Adriamycin-induced changes of creatine kinase activity in vivo and in cardiomyocyte culture, Toxicology 134(1) (1999) 51–62. [PubMed: 10413188]

[18]. Jungsuwadee P, Cole MP, Sultana R, Joshi G, Tangpong J, Butterfield DA, St Clair DK, Vore M, Increase in Mrp1 expression and 4-hydroxy-2-nonenal adduction in heart tissue of Adriamycin-treated C57BL/6 mice, Molecular cancer therapeutics 5(11) (2006) 2851–60. [PubMed: 17121932]

[19]. Griscavage JM, Wilk S, Ignarro LJ, Inhibitors of the proteasome pathway interfere with induction of nitric oxide synthase in macrophages by blocking activation of transcription factor NF-kappa B, Proceedings of the National Academy of Sciences of the United States of America 93(8) (1996) 3308–12. [PubMed: 8622934]

[20]. Keeney JT, Forster S, Sultana R, Brewer LD, Latimer CS, Cai J, Klein JB, Porter NM, Allan Butterfield D, Dietary vitamin D deficiency in rats from middle to old age leads to elevated tyrosine nitration and proteomics changes in levels of key proteins in brain: Implications for low vitamin D-dependent age-related cognitive decline, Free Radic Biol Med 65C (2013) 324–334.

[21]. Chandel NS, Trzyna WC, McClintock DS, Schumacker PT, Role of oxidants in NF-kappa B activation and TNF-alpha gene transcription induced by hypoxia and endotoxin, J Immunol 165(2) (2000) 1013–21. [PubMed: 10878378]

[22]. Kitamura Y, Hattori S, Yoneda S, Watanabe S, Kanemoto E, Sugimoto M, Kawai T, Machida A, Kanzaki H, Miyazaki I, Asanuma M, Sendo T, Doxorubicin and cyclophosphamide treatment produces anxiety-like behavior and spatial cognition impairment in rats: Possible involvement of hippocampal neurogenesis via brain-derived neurotrophic factor and cyclin D1 regulation, Behav Brain Res 292 (2015) 184–93. [PubMed: 26057360]

[23]. Kesler S, Janelsins M, Koovakkattu D, Palesh O, Mustian K, Morrow G, Dhabhar FS, Reduced hippocampal volume and verbal memory performance associated with interleukin-6 and tumor necrosis factor-alpha levels in chemotherapy-treated breast cancer survivors, Brain Behav Immun 30 Suppl (2013) S109–16. [PubMed: 22698992]

[24]. Kwatra M, Jangra A, Mishra M, Sharma Y, Ahmed S, Ghosh P, Kumar V, Vohora D, Khanam R, Naringin and Sertraline Ameliorate Doxorubicin-Induced Behavioral Deficits Through Modulation of Serotonin Level and Mitochondrial Complexes Protection Pathway in Rat Hippocampus, Neurochem Res 41(9) (2016) 2352–66. [PubMed: 27209303]

[25]. Bradford MM, A rapid and sensitive method for the quantitation of microgram quantities of protein utilizing the principle of protein-dye binding, Analytical biochemistry 72 (1976) 248–54. [PubMed: 942051]

[26]. Fang J, Seki T, Maeda H, Therapeutic strategies by modulating oxygen stress in cancer and inflammation, Advanced drug delivery reviews 61(4) (2009) 290–302. [PubMed: 19249331]

[27]. Mattiazzi M, D'Aurelio M, Gajewski CD, Martushova K, Kiaei M, Beal MF, Manfredi G, Mutated human SOD1 causes dysfunction of oxidative phosphorylation in mitochondria of transgenic mice, The Journal of biological chemistry 277(33) (2002) 29626–33. [PubMed: 12050154]

[28]. Naressi A, Couturier C, Castang I, de Beer R, Graveron-Demilly D, Java-based graphical user interface for MRUI, a software package for quantitation of in vivo/medical magnetic resonance spectroscopy signals, Comput Biol Med 31(4) (2001) 269–86. [PubMed: 11334636]

[29]. Keeney JTR, Ren X, Warrier G, Noel T, Powell DK, Brelsfoard JM, Sultana R, Saatman KE, Clair DKS, Butterfield DA, Doxorubicin-induced elevated oxidative stress and neurochemical alterations in brain and cognitive decline: protection by MESNA and insights into mechanisms of chemotherapy-induced cognitive impairment ("chemobrain"), Oncotarget 9(54) (2018) 30324–30339. [PubMed: 30100992]

[30]. Joshi G, Sultana R, Tangpong J, Cole MP, St Clair DK, Vore M, Estus S, Butterfield DA, Free radical mediated oxidative stress and toxic side effects in brain induced by the anti cancer drug adriamycin: insight into chemobrain, Free Radic Res 39(11) (2005) 1147–54. [PubMed: 16298740]

[31]. Keeney JT, Ren X, Warrier G, Noel T, Powell DK, Brelsfoard JM, Saatman KE, Sultana R, St Clair DK, Butterfield DA, Doxorubicin-induced elevated oxidative stress in brain and cognitive decline: protection by MESNA and insights into mechanisms of chemotherapy-induced cognitive impairment ("chemobrain"). In Press (2014).

[32]. Raffa RB, Tallarida RJ, Chemo fog: cancer chemotherapy-related cognitive impairment. Preface, Advances in experimental medicine and biology 678 (2010) vii–viii. [PubMed: 20737998]

[33]. Konat GW, Kraszpulski M, James I, Zhang HT, Abraham J, Cognitive dysfunction induced by chronic administration of common cancer chemotherapeutics in rats, Metab Brain Dis 23(3) (2008) 325–33. [PubMed: 18690526]

[34]. Chaturvedi RK, Flint Beal M, Mitochondrial diseases of the brain, Free Radic Biol Med 63 (2013) 1–29. [PubMed: 23567191]

[35]. Butterfield DA, Perluigi M, Reed T, Muharib T, Hughes CP, Robinson RA, Sultana R, Redox proteomics in selected neurodegenerative disorders: from its infancy to future applications, Antioxidants & redox signaling 17(11) (2012) 1610–55. [PubMed: 22115501]

[36]. Siegel GJ, Basic neurochemistry : molecular, cellular, and medical aspects, 7th ed., Elsevier, Amsterdam; Boston, 2006.

[37]. Jansen JF, Backes WH, Nicolay K, Kooi ME, 1H MR spectroscopy of the brain: absolute quantification of metabolites, Radiology 240(2) (2006) 318–32. [PubMed: 16864664]

[38]. Meck WH, Church RM, Matell MS, Hippocampus, time, and memory-A retrospective analysis, Behavioral neuroscience 127(5) (2013) 642–54. [PubMed: 24128354]

[39]. Goulart BK, de Lima MN, de Farias CB, Reolon GK, Almeida VR, Quevedo J, Kapczinski F, Schroder N, Roesler R, Ketamine impairs recognition memory consolidation and prevents learning-induced increase in hippocampal brain-derived neurotrophic factor levels, Neuroscience 167(4) (2010) 969–73. [PubMed: 20338225]

[40]. Clarke JR, Cammarota M, Gruart A, Izquierdo I, Delgado-Garcia JM, Plastic modifications induced by object recognition memory processing, Proceedings of the National Academy of Sciences of the United States of America 107(6) (2010) 2652–7. [PubMed: 20133798]

[41]. Sarkisyan G, Hedlund PB, The 5-HT7 receptor is involved in allocentric spatial memory information processing, Behav Brain Res 202(1) (2009) 26–31. [PubMed: 19447277]

[42]. Mallampalli RK, Ryan AJ, Salome RG, Jackowski S, Tumor necrosis factor-alpha inhibits expression of CTP:phosphocholine cytidylyltransferase, The Journal of biological chemistry 275(13) (2000) 9699–708. [PubMed: 10734122]

[43]. Church LD, Hessler G, Goodall JE, Rider DA, Workman CJ, Vignali DA, Bacon PA, Gulbins E, Young SP, TNFR1-induced sphingomyelinase activation modulates TCR signaling by impairing store-operated Ca2+ influx, Journal of leukocyte biology 78(1) (2005) 266–78. [PubMed: 15817701]

[44]. Soares DP, Law M, Magnetic resonance spectroscopy of the brain: review of metabolites and clinical applications, Clinical radiology 64(1) (2009) 12–21. [PubMed: 19070693]

[45]. Bertholdo D, Watcharakorn A, Castillo M, Brain proton magnetic resonance spectroscopy: introduction and overview, Neuroimaging clinics of North America 23(3) (2013) 359–80. [PubMed: 23928194]

[46]. Ciszkowska-Lyson B, Krolicki L, Teska A, Janowicz-Zebrowska A, Krzakowski M, Tacikowska M, [Brain metabolic disorders after chemotherapy in the study by magnetic resonance spectroscopy], Neurologia i neurochirurgia polska 37(4) (2003) 783–98. [PubMed: 14746239]

[47]. Tabaczar S, Czepas J, Koceva-Chyla A, Kilanczyk E, Piasecka-Zelga J, Gwozdzinski K, The effect of the nitroxide pirolin on oxidative stress induced by doxorubicin and taxanes in the rat brain, J Physiol Pharmacol 68(2) (2017) 295–308. [PubMed: 28614779]

[48]. Banks WA, From blood-brain barrier to blood-brain interface: new opportunities for CNS drug delivery, Nat Rev Drug Discov 15(4) (2016) 275–92. [PubMed: 26794270]

[49]. Lien YC, Noel T, Liu H, Stromberg AJ, Chen KC, St Clair DK, Phospholipase C-delta1 is a critical target for tumor necrosis factor receptor-mediated protection against adriamycin-induced cardiac injury, Cancer research 66(8) (2006) 4329–38. [PubMed: 16618758]

[50]. Lee SM, Choi HJ, Oh CH, Oh JW, Han JS, Leptin increases TNF-alpha expression and production through phospholipase D1 in Raw 264.7 cells, PLoS One 9(7) (2014) e102373. [PubMed: 25047119]

[51]. De Valck D, Beyaert R, Van Roy F, Fiers W, Tumor necrosis factor cytotoxicity is associated with phospholipase D activation, Eur J Biochem 212(2) (1993) 491–7. [PubMed: 8444187]

[52]. Friday SC, Fox DA, Phospholipase D enzymes facilitate IL-17- and TNFalpha-induced expression of proinflammatory genes in rheumatoid arthritis synovial fibroblasts (RASF), Immunol Lett 174 (2016) 9–18. [PubMed: 27058440]

[53]. Urbahn MA, Kaup SC, Reusswig F, Kruger I, Spelleken M, Jurk K, Klier M, Lang PA, Elvers M, Phospholipase D1 regulation of TNF-alpha protects against responses to LPS, Sci Rep 8(1) (2018) 10006. [PubMed: 29968773]

[54]. Zhang F, Zhao G, Dong Z, Phosphatidylcholine-specific phospholipase C and D in stimulation of RAW264.7 mouse macrophage-like cells by lipopolysaccharide, Int Immunopharmacol 1(7) (2001) 1375–84. [PubMed: 11460317]

[55]. Oprins JC, van der Burg C, Meijer HP, Munnik T, Groot JA, Tumour necrosis factor alpha potentiates ion secretion induced by histamine in a human intestinal epithelial cell line and in mouse colon: involvement of the phospholipase D pathway, Gut 50(3) (2002) 314–21. [PubMed: 11839707]

[56]. Jang YH, Ahn BH, Namkoong S, Kim YM, Jin JK, Kim YS, Min do S, Differential regulation of apoptosis by caspase-mediated cleavage of phospholipase D isozymes, Cellular signalling 20(12) (2008) 2198–207. [PubMed: 18694819]

[57]. Nakashima S, Nozawa Y, Possible role of phospholipase D in cellular differentiation and apoptosis, Chemistry and physics of lipids 98(1–2) (1999) 153–64. [PubMed: 10358937]

[58]. Jang YH, Namkoong S, Kim YM, Lee SJ, Park BJ, Min DS, Cleavage of phospholipase D1 by caspase promotes apoptosis via modulation of the p53-dependent cell death pathway, Cell death and differentiation 15(11) (2008) 1782–93. [PubMed: 18636075]

[59]. Nozawa Y, Roles of phospholipase D in apoptosis and pro-survival, Biochimica et biophysica acta 1585(2–3) (2002) 77–86. [PubMed: 12531540]

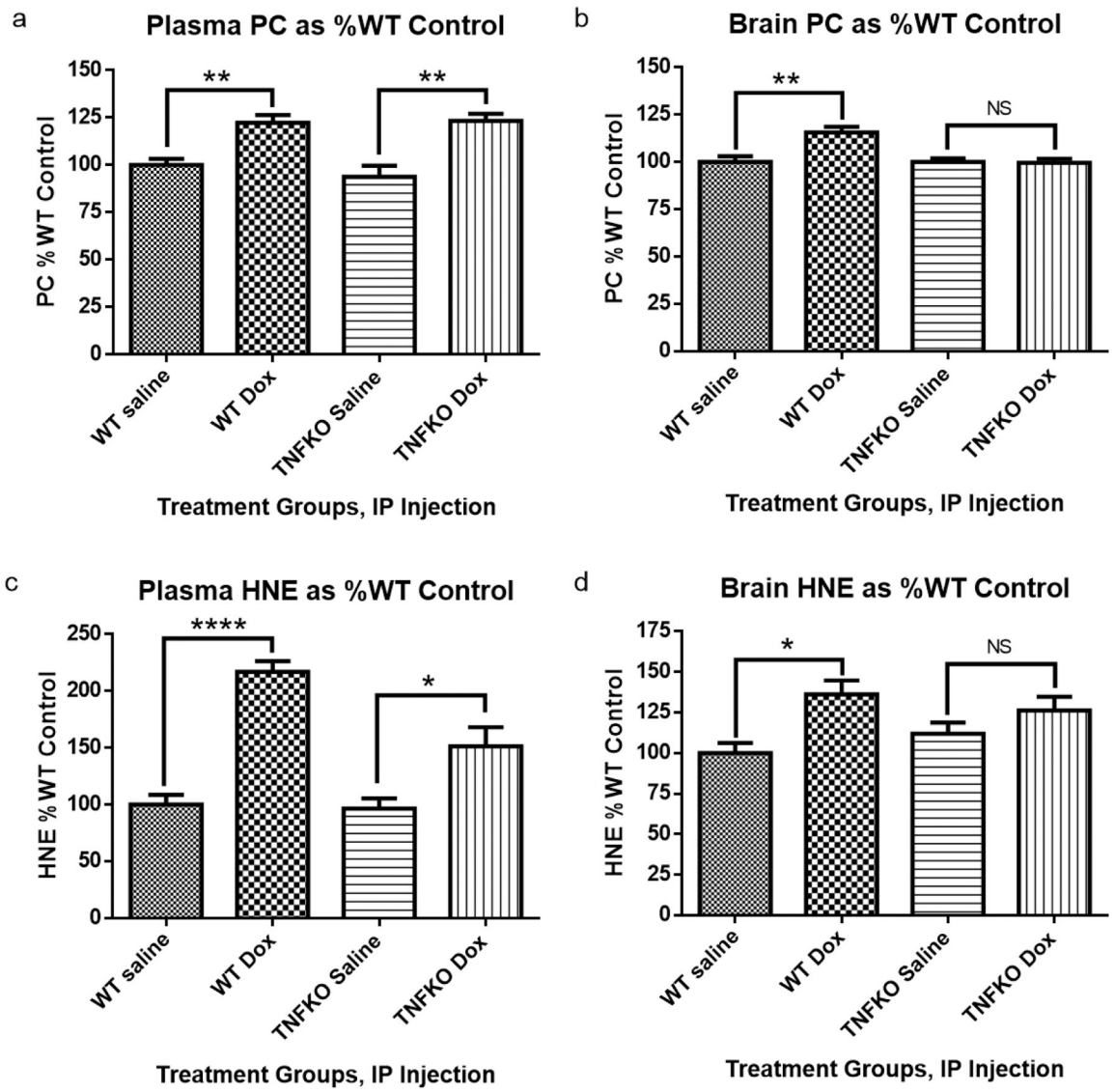

Fig. 1.

Protein carbonyl (PC) and protein-bound HNE (HNE) are measures of protein oxidation and lipid peroxidation, respectively. Samples were collected approximately 72 h following treatment. (**a**) PC levels in plasma were significantly elevated following Dox administration of both WT and tumor necrosis factor-alpha knockout (TNFKO) mice compared to saline-treated mice. (**b**) PC levels in brain were significantly elevated following Dox treatment in WT mice; however, PC levels in brain of TNFKO mice were statistically unchanged from those observed in saline-treated WT and TNFKO mice. (**c**) Dox administration resulted in significant elevation of protein-bound HNE in both plasma and brain of WT mice. (**d**) In TNFKO mice, protein-bound HNE levels were significantly elevated in plasma; however, protein-bound HNE levels in brain were not significantly different than levels observed in brains from saline-treated WT or TNFKO mice. (n=6 individually employed mice per treatment group; *p<0.05, **p<0.01, ***p<0.001, ****p<0.0001, NS = not significant).

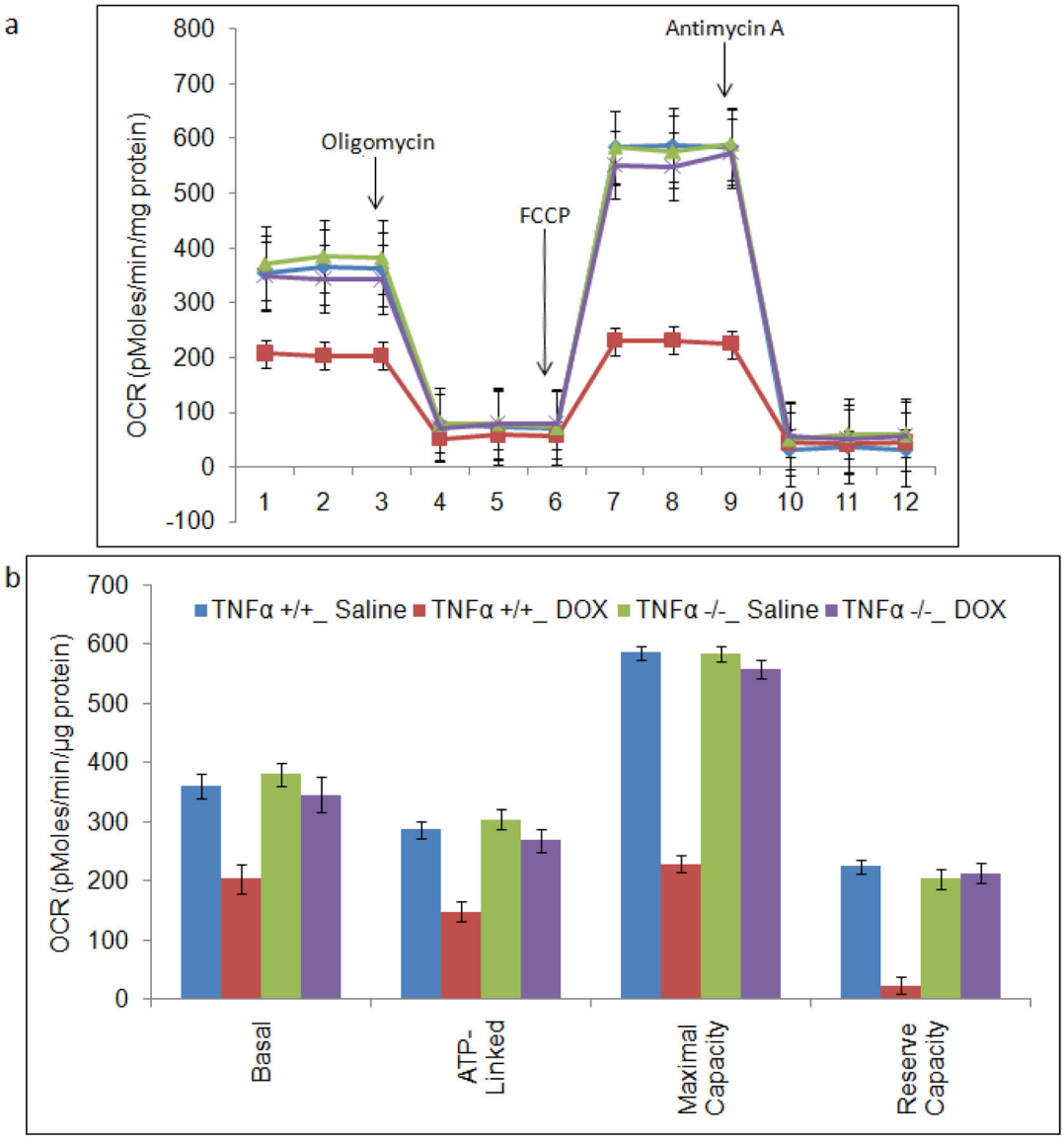

Fig. 2.

Measurement of mitochondrial function in brain mitochondria using the Seahorse XF96 analyzer. Mitochondrial protein (5 µg) were plated into wells of Seahorse Bioscience tissue culture plates and centrifuged before the measurement of total oxygen consumption rate (OCR). Mitochondrial oxygen consumption rate (OCR) in brain mitochondria is indicated as brain mitochondria from: saline-treated WT (blue circles); Dox-treated WT (red squares; saline-treated TNFKO (purple x's); and Dox-treated TNFKO (green triangles). (**a**) For each sample, OCRs were measured at four time points in real time and plotted as a function of cells under the basal condition followed by the sequential addition in different wells of Oligomycin (1µg/ml), FCCP (3µM) and Antimycin (2µM). (**b**) Quantification showing the relative contribution of oxygen consumption, ATP-linked oxygen consumption, the maximal OCR after the addition of FCCP, and the reserve capacity of the mitochondria. All data are

shown as the Mean±SEM of triplicate samples and are representative of 3 independent experiments (n=3).

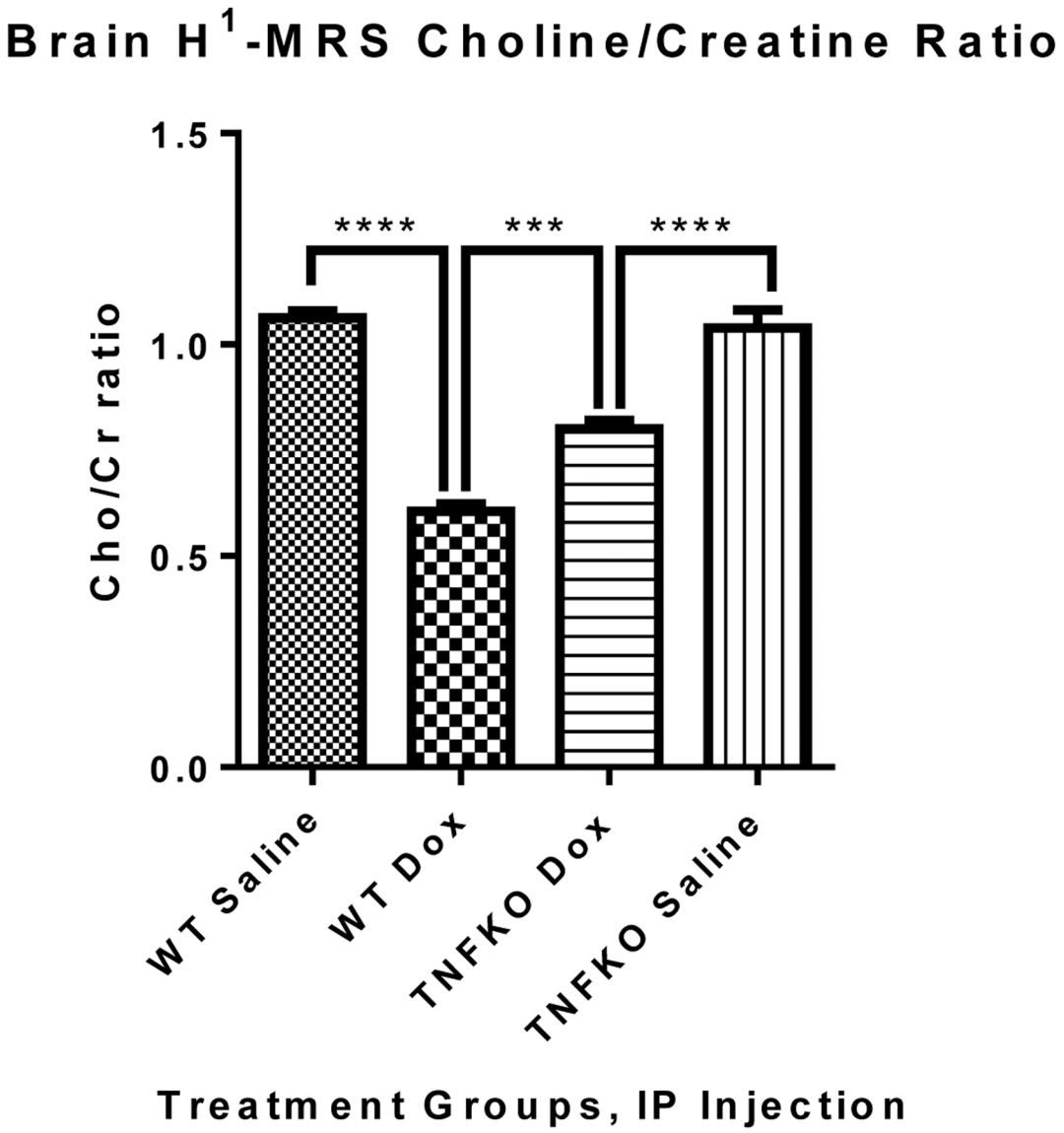

Fig. 3.

Bilateral H^1-MRS scans of hippocampus revealed a large decrease in the Cho/Cr ratio in the Dox-treated WT group compared to saline control mice (****$p<0.0001$). Dox administration to TNFKO mice resulted in rebound of the hippocampal Cho/Cr ratio over that of Dox-treated WT mice (***$p=0.0002$), although there also was a significant difference in the Cho/Cr ratio in mice hippocampus of TNFKO mice between saline and Dox treatment groups (****$P<0.0001$). (n=6 and 5 individual animals of the WT and TNFKO groups, respectively).

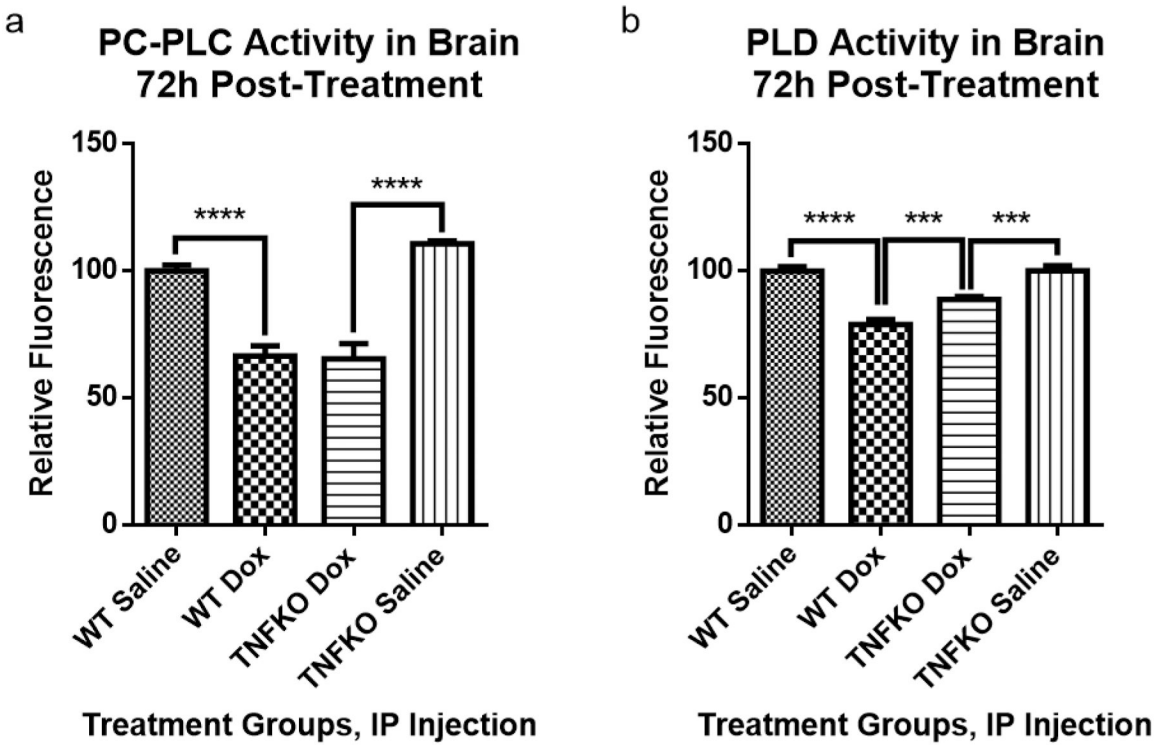

Fig. 4.

Brain phosphatidylcholine-specific phospholipase C (PC-PLC) and phospholipase D (PLD) activity assays were performed at room temperature in the dark according to the manufacturers' instructions. The data are presented as percent saline control. (**a**) PC-PLC activity was measured after 22.5h of incubation of assay reagents and samples, the time at which the fluorescence of the corresponding positive control was maximum. Cleavage of the assay substrate by PC-PLC yields a dye-labeled diacylglycerol (DAG) that fluoresces using excitation and emission wavelength maxima of 509 and 516nm, respectively. Dox administration to WT mice caused a significant decrease in PC-PLC activity compared to saline treated WT mice (****$p<0.0001$). Dox treatment of TNFKO mice resulted in similar decrease in PC-PLC activity compared to saline treated TNFKO mice (****$p<0.0001$). (**b**) Brain PLD activity at 1h of incubation of assay reagents and samples, the time of maximal fluorescence of the corresponding positive control in these trials, was performed according to manufacturer's instructions at 37°C protected from light. PLD cleaves the alcohol component of the head group of phospholipids thereby releasing the choline from PtdCho. Assay reactions involving the choline produce a product that fluoresces using excitation and emission wavelength maxima of 571 and 585nm, respectively. Dox treatment resulted in significantly decreased PLD activity in WT mice brain compared to that of saline-treated WT mice (****$p<0.0001$). Dox treatment also resulted in significantly decreased PLD activity in TNFKO mice brain compared to that of saline-treated TNFKO mice (***$P=0.0005$). However, PLD activity was preserved in Dox-treated TNFKO mice, significantly higher than PLD activity in brain of Dox-treated WT mice (***$p=0.0008$). (For determination of PC-PLC activity, n=6 for all groups except for the saline-treated TNFKO

group n=7; for determination of PLD activity, n=9, 10, 11 and 7 for WT saline, WT Dox, TNFKO Dox and TNFKO saline groups, respectively).

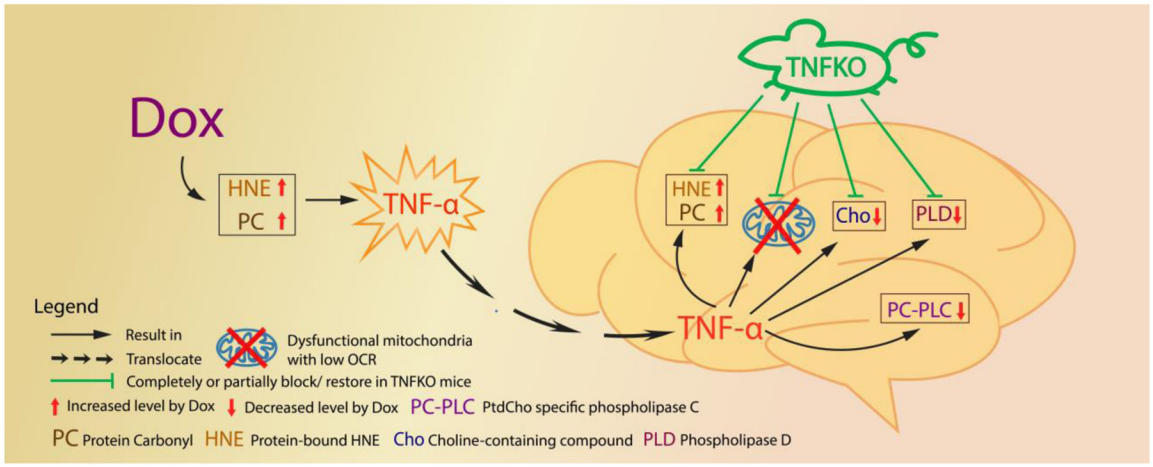

Fig. 5.

Schematic illustration of the sequelae of events in brain following Dox treatment of mice and their prevention or modulation in mice lacking the gene for *TNF-α*. The red arrows represent the changes following Dox administration in mice observed in present study and the green lines represent that most of these changes are completely or partially prevented in TNFKO mice.